Original Article

Structure, spectral analysis and microwave dielectric properties of novel x(NaBi)$_{0.5}$MoO$_4$-(1-x)Bi$_{2/3}$MoO$_4$ ($x = 0.2 \sim 0.8$) ceramics with low sintering temperatures

Shu-Zhao Hao[a], Di Zhou[a,*], Fayaz Hussain[b], Wen-Feng Liu[c], Jin-Zhan Su[d], Da-Wei Wang[e], Qiu-Ping Wang[f], Ze-Ming Qi[g], Charanjeet Singh[h], Sergei Trukhanov[i,j,k]

[a] Electronic Materials Research Laboratory, Key Laboratory of the Ministry of Education & International Center for Dielectric Research, School of Electronic Science and Engineering, Xi'an Jiaotong University, Xi'an, 710049, China
[b] Department of Materials Engineering, NED University of Engineering & Technology, Karachi, 75270, Pakistan
[c] State Key Laboratory of Electrical Insulation and Power Equipment, Xi'an Jiaotong University, Xi'an 710049, Shaanxi, China
[d] International Research Centre for Renewable Energy, State Key Laboratory of Multiphase Flow in Power Engineering, Xi'an Jiaotong University, Xi'an, Shaanxi 710049, China
[e] Department of Materials Science and Engineering, University of Sheffield, Sheffield S1 3JD, United Kingdom
[f] School of Science, Xi'an Polytechnic University, Xi'an, 710048, China
[g] National Synchrotron Radiation Laboratory, University of Science and Technology of China, Hefei, Anhui 230029, China
[h] School of Electronics and Communication Engineering, Lovely Professional University, Jalandhar, Punjab, India
[i] National University of Science and Technology "MISiS", Leninskii Av., 4, Moscow, 4119049, Russia
[j] South Ural State University, Lenin Av., 76, Chelyabinsk, 454080, Russia
[k] Scientific and Practical Materials Research Center of the NAS of Belarus, P. Brovki Str., 19, Minsk, 220072, Belarus

ARTICLE INFO

ABSTRACT

Herein, the x(NaBi)$_{0.5}$MoO$_4$-(1-x)Bi$_{2/3}$MoO$_4$ (xNBM-(1-x)BMO, $x = 0.2 \sim 0.8$) microwave dielectric ceramics with low sintering temperatures were prepared via the traditional solid-state method to adjust the τ_f value and dielectric constant. The crystal structure was determined using X-Ray diffraction and Raman spectroscopy, the microstructure was investigated using scanning electron micrograph and energy disperse spectroscopy, and the dielectric properties were studied using a network analyser and infrared spectroscopy. For the xNBM-(1-x)BMO composite ceramics, the (NaBi)$_{0.5}$MoO$_4$ tetragonal phase coexisted with the Bi$_{2/3}$MoO$_4$ monoclinic phase. With the rise of x value, the permittivity increased from 23.7–29.8, and the τ_f value shifted from -53.3 ppm/°C to -13.7 ppm/°C. The 0.8NBM-0.2BMO ceramic sintered at 680 °C possessed excellent microwave dielectric properties with a ε_r = 29.8 (6.7 GHz), a Qf = 11,800 GHz, and a τ_f = -13.7 ppm/°C. These results made the xNBM-(1-x)BMO composite ceramics great candidates in low temperature co-fired ceramics technology.

1. Introduction

The investigation of microwave dielectric materials is closely related to the development of modern mobile communication systems, and various microwave dielectric ceramics are used at different frequency bands. Currently, 5th generation wireless systems have received increasing attention from both industry and researchers, especially the investigation of microwave devices applied at the millimetre wave band. Furthermore, due to the requirements of different fields of communication technology, microwave dielectric materials with different permittivities are required to produce various microwave devices [1–4]. Recently, the novel ceramic fabrication technology, low-temperature co-fired ceramic (LTCC) technology, has provided technical support for the fabrication of integrated microwave devices. Microwave components and devices can be massively manufactured using LTCC technology, and it helps integrate and minimize the dimension of devices. For example, the devices used in Massive MIMO (multiple input multiple output) need to be largely produced with LTCC technology [5]. To be employed in LTCC technology, microwave dielectric ceramics must meet the following requirements. First, considering that the metal electrode has a low melting temperature (such as Ag with MP 961 °C), the microwave materials need an intrinsic low-firing temperature to co-fire with the electrode. Second, a suitable permittivity is an important factor for the microwave devices with certain dimensions.

---

* Corresponding author.
  E-mail address: zhoudi1220@gmail.com (D. Zhou).

Please cite this article as: Shu-Zhao Hao, et al., Journal of the European Ceramic Society, https://doi.org/10.1016/j.jeurceramsoc.2020.03.074

Third, the near-zero τ_f value is another indispensable performance parameter for microwave devices to work stably at various operating temperatures. Finally, the raw materials should be non-hazardous for environmental protection [6–10]. Hence, microwave materials with low firing temperatures, various permittivities high Qf values (Q = 1/dielectric loss; f = resonant frequency) and near-zero τ_f values might be used in LTCC technologies.

Recently, many excellent microwave materials with low sintering temperatures have been reported in Bi-rich, Li-rich, V-rich and Mo-rich materials. Fang et al. found that LiMVO$_6$ (M = Mo, W) ceramics could densify below 700 °C and display favourable microwave dielectric properties (ε_r = 11.5 and 13.3, Qf = 12,460 and 13,260 GHz, τ_f = +101 and +168.8 ppm/°C) [11]. Udovic et al. used the Bi$_2$O$_3$-TeO$_2$ system to prepare a series of microwave ceramics sintered below 800 °C, and these ceramics showed good dielectric properties (ε_r = 30 ~ 54, Qf = 1,100 ~ 41,000 GHz, τ_f = -43 ~ -144 ppm/°C) [12]. Tellurates and vanadates have toxic components that are not environmentally friendly, many researchers have given more attention to Mo-based microwave ceramics. Since phase diagrams are very useful for the development of microwave materials, Zhou et al. used the Bi$_2$O$_3$-MoO$_3$ two-phase diagram and found a battery of ceramics with excellent microwave dielectric properties: Bi$_2$MoO$_6$ sintered at 750 °C with ε_r = 31, Qf = 16,700 GHz and τ_f = -114 ppm/°C; Bi$_2$Mo$_2$O$_9$ sintered at 620 °C with ε_r = 38, Qf = 12,500 GHz and τ_f = +31 ppm/°C; Bi$_2$Mo$_3$O$_{12}$ sintered at 610 °C with ε_r = 19, Qf = 21,800 GHz and τ_f = -215 ppm/°C [13]. Later, it was found that many A^{2+}B^{6+}O$_4$ oxides with scheelite structures have low sintering temperatures and flexible microstructures to improve the microwave dielectric properties of ceramics [14–17]. Zhou et al. reported the (ABi)$_{0.5}$MoO$_4$ (A = Ag, Na) ceramic sintered at 690 °C with high-performance dielectric properties (ε_r = 30.4 and 34.4, Qf = 12,600 and 12,300 GHz, τ_f = +57 and +43 ppm/°C) [18]. The phase analysis of the ceramics is very important, and the microstructure of microwave ceramics is closely related to the microwave properties. Many tools are applied to conduct supporting studies. Raman spectroscopy and Fourier transform infrared spectroscopy are very useful tools to study ceramic material microstructure and analyse the dielectric response occurring in internal ceramics. With Raman spectroscopy, all the vibration modes between different ions can be gained, and this information is valid evidence to reveal the micromechanism in the ceramic material [19,20]. Moreover, according to the fitted infrared spectrum, the intrinsic dielectric effect determined by the polar optical phonon could be revealed [21,22]. In this work, based on the Na$_2$O-Bi$_2$O$_3$-MoO$_3$ ternary phase diagram, a series of x(NaBi)$_{0.5}$MoO$_4$-(1-x)Bi$_{2/3}$MoO$_4$ (xNBM-(1-x)BMO, x = 0.2 ~ 0.8) ceramics were prepared using conventional synthesis. The crystalline phase, micro-morphology, and dielectric properties were investigated with the volume ratio of the composition.

2. Experimental procedure

A series of x(NaBi)$_{0.5}$MoO$_4$-(1-x)Bi$_{2/3}$MoO$_4$ (xNBM-(1-x)BMO, x = 0.2 ~ 0.8) ceramics was proportionally synthesised using the high-purity materials Bi$_2$O$_3$ (> 99 %), Na$_2$CO$_3$ (> 99 %), and MoO$_3$ (> 99.95 %). The preparative powders were mixed with alcohol using a planetary ball mill for 4 h, and the dried powders were calcined at 550 °C for 4 ~ 6 h. Then, the calcined powders were crudely crushed using a mortar and finely ground using a ball mill for 4 h. The wet powders were dried in a oven for 12 h. Then PVA binder was added to the powders, and the powders were granulated. Finally, these materials were put into a steel die and pressed into cylinders using a hydropress. The height and diameter of the samples are 4 mm and 10 mm, respectively. In addition, the pressure applied to the sample is 100 MPa. All the samples were sintered in a muffle furnace, and the sintering temperature ranged from 620 °C to 680 °C for 2 h.

Room temperature XRD was applied to identify the crystalline phase of the ceramics, and the radiation was from a Cu Kα source. The surface

and fracture features of the ceramic were observed using scanning electron microscopy (SEM). Raman spectra were measured using a Raman spectrometer. An Ar$^+$ laser (514.5 nm) was applied as a pumping source with a power of 20 mW. IR reflectivity spectra were collected on polished pellets using a Bruker Optik IFS 66v FTIR spectrometer (IFS 66v/S Vacuum; Bruker Optik GmbH, Germany). The bulk densities of the xNBM-(1-x)BMO ceramics are measured by the Archimedes principle. The dielectric properties of the samples were measured using a network analyser (8720ES, Agilent, Palo Alto, CA), and the calculated data were obtained with the TE$_{01\delta}$ shielded cavity method. A temperature chamber (Delta 9023, Delta Design, Poway, CA) connected with the network analyser was used to test the temperature coefficient of resonant frequency (τ_f value). The testing temperature ranged from 25 °C to 85 °C, and the τ_f value was calculated with the following formula:

$$\tau_f = \frac{f_{85} - f_{25}}{f_{25}(85-25)} \times 10^6 ppm/^oC \tag{1}$$

where f$_{85}$ is the TE$_{01\delta}$ resonant frequency at 85 °C and f$_{25}$ is the TE$_{01\delta}$ resonant frequency at 25 °C.

3. Results and discussions

All the compositions of the xNBM-(1-x)BMO ceramics (x = 0.2 ~ 0.8) are located in the Na$_2$O-Bi$_2$O$_3$-MoO$_3$ ternary phase diagram as shown in Fig. 1. In this ternary phase diagram, Zhou et al. studied the Bi$_2$O$_3$-MoO$_3$ binary system and found a series of microwave ceramics (Bi$_2$Mo$_3$O$_{12}$, Bi$_2$Mo$_2$O$_9$, Bi$_2$MoO$_6$) with favourable dielectric properties. [13] Zhang et al. studied a series of Na$_2$O-MoO$_3$ binary materials, such as Na$_6$Mo$_{11}$O$_{36}$, Na$_2$Mo$_2$O$_7$, Na$_2$MoO$_4$, with good microwave dielectric properties. [23] The powder diffraction patterns of these ceramics sintered at their optimal temperature are shown in Fig. 2. In the XRD patterns, the peaks indexed as the tetragonal phase are derived from the (NaBi)$_{0.5}$MoO$_4$ ceramic, [24] and the other peaks indexed as the monoclinic phase are derived from the Bi$_{2/3}$MoO$_4$ (Bi$_2$Mo$_3$O$_{12}$) ceramic. [25] These two phases were found to coexist with each other, and all the peaks corresponded well with the PDF card (No.21−0103) and PDF card (No.51–1508). As shown in the enlarged image in Fig. 2, when x value increases, the intensities of the (-221), (023), (100) and (012) peaks of the Bi$_{2/3}$MoO$_4$ ceramic gradually decrease, while the intensities of the (112), (004) and (204) peaks of the (NaBi)$_{0.5}$MoO$_4$ ceramic increase. Furthermore, only the peaks of the (NaBi)$_{0.5}$MoO$_4$ ceramic and Bi$_{2/3}$MoO$_4$ ceramic can be observed in the XRD patterns. Hence, a series of xNBM-(1-x)BMO composite ceramics have been successfully prepared without extra phases. In addition, crystal structures of the (NaBi)$_{0.5}$MoO$_4$ and Bi$_{2/3}$MoO$_4$ ceramics are shown in inset in Fig. 2. The (NaBi)$_{0.5}$MoO$_4$ ceramic belongs to a tetragonal scheelite phase with (NaBi) ions occupying the A-site, and the Bi$_{2/3}$MoO$_4$ ceramic is a monoclinic phase with a Bi^{3+} ion occupying the A-site.

SEM micrographs of the xNBM-(1-x)BMO (x = 0.2 ~ 0.8) ceramics sintered at different temperatures are shown in Fig. 3(a∼d) and the polished surface of 0.8NBM-0.2BMO ceramic after thermal etching is shown in Fig. 3(e). As shown in Fig. 3(a), two phases are clearly observed in the 0.2NBM-0.8BMO ceramic, and small grains are distributed at the grain boundaries of the large ones. As x value increases, the xNBM-(1-x)BMO ceramics show a dense and homogeneous microstructure, and the small grains gradually disappear. The grain size of the large ones decreases from 8 ~ 10 μm to 3 ~ 5 μm. When x value reaches 0.8, as-fired surface of the 0.8NBM-0.2BMO ceramic only shows large grains. However, as seen from the thermally etched surfaces, it is clearly that two kinds of grains co-exist in the ceramics.

For a further study on the existence of two phases in 0.8NBM-0.2BMO ceramic, the cross-section of the 0.8NBM-0.2BMO ceramic is investigated. The SEM image of the cross-section of the 0.8NBM-0.2BMO ceramic is shown in Fig. 4(a) and the SEM image of the
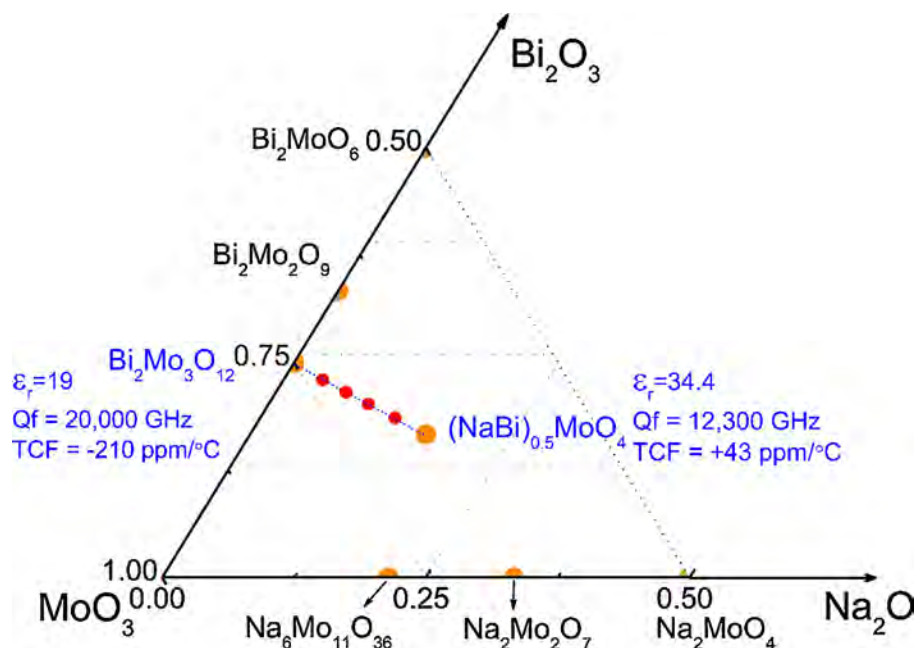
Fig. 1. The xNBM-(1-x)BMO (x = 0.2 ~ 0.8) (red circle) ceramics in the Na_2O-Bi_2O_3-MoO_3 ternary phase diagram.

0.8NBM-0.2BMO ceramic after thermal etching is shown in Fig. 4(b). Compared with the cross-section of 0.8NBM-0.2BMO ceramic in Fig. 4(a), when the polished sample is annealed at 610 °C, two kinds of grains appear in the polished cross-section of the 0.8NBM-0.2BMO ceramic in Fig. 4(b). Especially inset BS-SEM image in Fig. 4(b), this phenomenon can be clearly observed. According to the literature, [13] the sintering temperature of the $Bi_{2/3}MoO_4$ ceramic is 620 °C, and the annealing process causes $Bi_{2/3}MoO_4$ ceramic grain growth. From EDS analysis in Fig. 4(c ~ d), it can be seen that the large grains (e.g. Spot B) with a dark grey colour belong to the $(NaBi)_{0.5}MoO_4$ phase and the small grains (e.g. Spot A) with a bright white colour are identified as the $Bi_{2/3}MoO_4$ phase. However, these small grains still include Na element derived from the $(NaBi)_{0.5}MoO_4$. Hence, it can be concluded that the

$Bi_{2/3}MoO_4$ phase and $(NaBi)_{0.5}MoO_4$ phase may have partial solutions and the two phases coexist with each other. This phenomenon is similar to the XRD analysis above.

The Raman spectrum is a useful tool to confirm the phase of the ceramic and to provide information on the short-range characteristics in crystalline materials. From the analysis of XRD data, the xNBM-(1-x)BMO ceramics have two phases. The $(NaBi)_{0.5}MoO_4$ ceramic belongs to the scheelite structure with the $I4_{1/a}$ space group, and $Bi_{2/3}MoO_4$ belongs to the monoclinic structure with the $P2_1/c$ space group. According to the literature, [26] the $(NaBi)_{0.5}MoO_4$ ceramic with tetragonal structure has 26 vibration modes, and the calculated results are as follows:
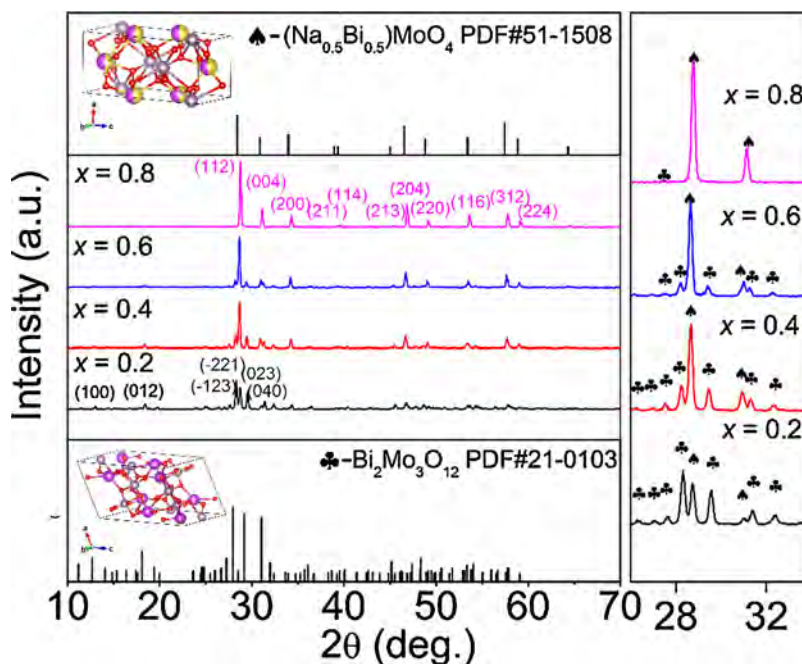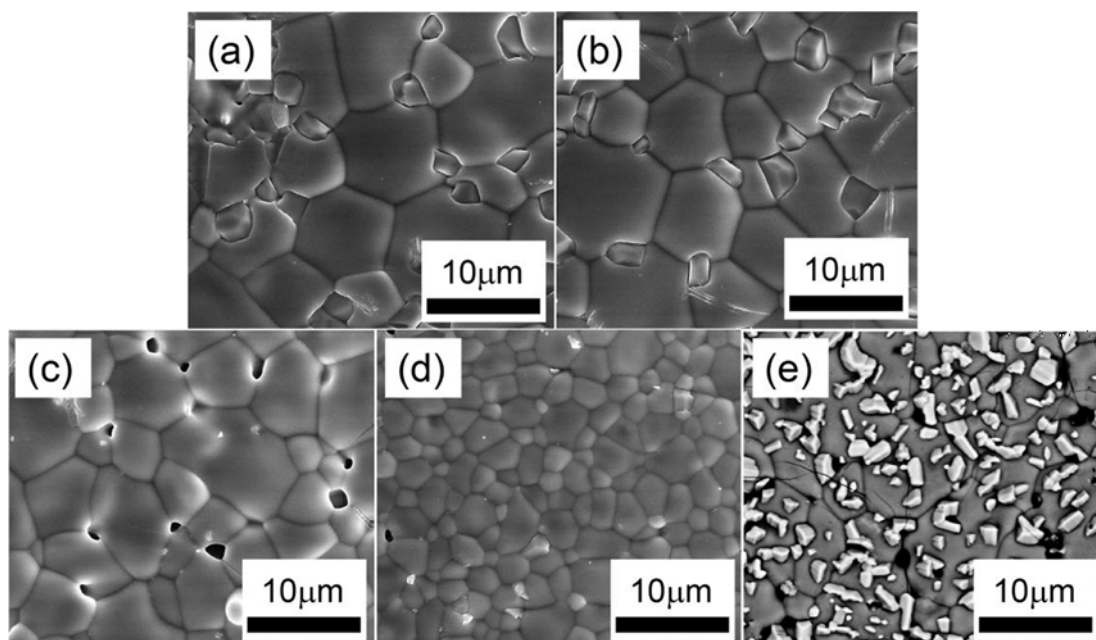

Fig. 2. XRD patterns of the xNBM-(1-x)BMO (x = 0.2 ~ 0.8) ceramics (♠ is $(NaBi)_{0.5}MoO_4$ and ♣ is $Bi_{2/3}MoO_4$ phase), the crystal structures of the $(NaBi)_{0.5}MoO_4$ ceramic (inset), the crystal structures of the $Bi_{2/3}MoO_4$ ceramic (inset).

Fig. 3. SEM images of surfaces of xNBM-(1-x)BMO ceramics sintered at different temperature (a) x = 0.2 (620 °C for 2 h), (b) x = 0.4 (640 °C for 2 h), (c) x = 0.6 (660 °C for 2 h), (d) x = 0.8 (680 °C for 2 h), (e) SEM images of polished surface of 0.8NBM-0.2BMO ceramic after thermal etching (610 °C for 2 h).
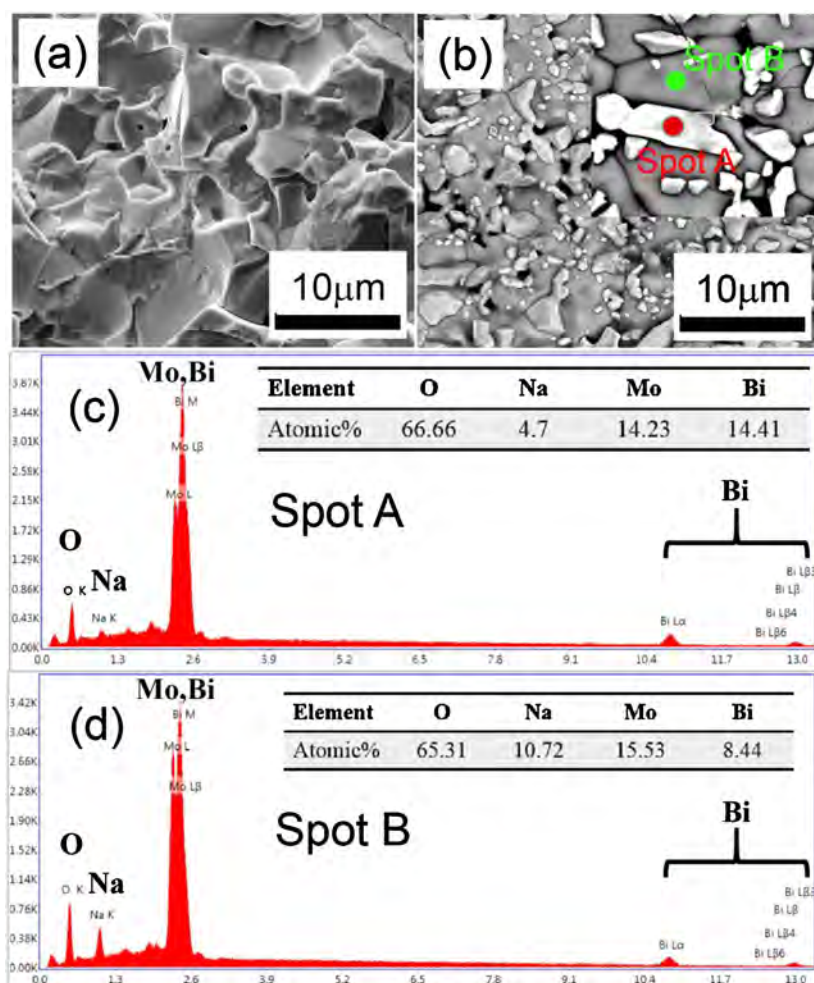
Fig. 4. (a) SEM image of cross-section without etching, (b) SEM image and BS-SEM image (inset) of polished cross-section with etching of 0.8NBM-0.2BMO ceramic, (c) and (d) EDS analysis of 0.8NBM-0.2BMO ceramic annealed at 610 °C for 2 h.
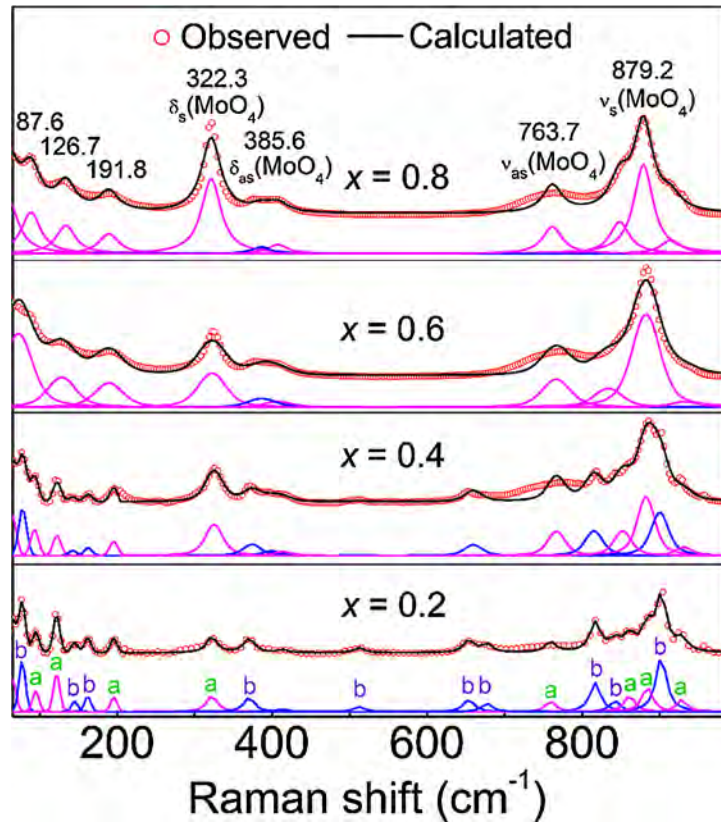
Fig. 5. The observed and calculated Raman spectroscopy of xNBM-(1-x)BMO (x = 0.2 ~ 0.8) ceramics (a the peaks of vibration modes came from the (NaBi)$_{0.5}$MoO$_4$, b the peaks of vibration modes came from the Bi$_{2/3}$MoO$_4$).

$$\Gamma = 3A_g + 5B_g + 5E_g + 5A_u + 5E_u + 3B_u \qquad (2)$$

All g modes are Raman-active; A$_u$ and E$_u$ are IR-active. As shown in Fig. 5, when x is 0.2, the strong peaks at 816.2 cm^{-1} and 903.7 cm^{-1} belong to the stretching vibrations, and the secondary strong peaks at 78.1 cm^{-1} and 123.2 cm^{-1} belong to the vibrations of A-site ions. These peaks all come from Bi$_{2/3}$MoO$_4$ (marked as b), while the vibrational modes of (NaBi)$_{0.5}$MoO$_4$ (marked as a) are also observed. This result indicates that the xNBM-(1-x)BMO ceramics are composed of two phases. When x is 0.8, the strongest vibrational mode near 879.2 cm^{-1} is assigned to the symmetric stretching vibration between Mo and O, and the weaker shoulder near 763.7 cm^{-1} is assigned to the antisymmetric Mo−O stretching mode. The next strong vibration mode near 324.8 cm^{-1} is assigned to the symmetric Mo-O bending vibration, and the peak near 385.6 cm^{-1} came from the anti-symmetric Mo-O bending vibration [27]. However, vibrational peaks from the Bi$_{2/3}$MoO$_4$ ceramic are too weak to be observed.

The Fourier transform infrared spectra of the xNBM-(1-x)BMO ceramics are shown in Fig. 6. When x value is 0.2, the peaks (marked as 1) of the vibrational modes at 93 cm^{-1}, 154 cm^{-1}, 304 cm^{-1}, 461 cm^{-1}, 545 cm^{-1}, 632 cm^{-1}, 696 cm^{-1}, 717 cm^{-1}, and 931 cm^{-1} all belong to the IR vibration of the Bi$_{2/3}$MoO$_4$ ceramic, and the intensities of these peaks are very strong; moreover, the peaks from the (NaBi)$_{0.5}$MoO$_4$ are also observed. As x value increases, the peaks from the Bi$_{2/3}$MoO$_4$ ceramic decrease. When x value is 0.8, the peaks (marked as 2) of the vibrational modes at 84 cm^{-1}, 129 cm^{-1}, 167 cm^{-1}, 258 cm^{-1}, 309 cm^{-1}, 399 cm^{-1}, 727 cm^{-1}, 776 cm^{-1}, 835 cm^{-1}, and 901 cm^{-1} all belong to the IR vibration of the (NaBi)$_{0.5}$MoO$_4$ ceramic. The number of vibrational modes decreases due to the reduction of Bi$_{2/3}$MoO$_4$ ceramic.

The fitted infrared spectra of xNBM-(1-x)BMO ceramics based on the classical harmonic oscillator model employs the Lorentz formula [Eq. (3)] to analyse the complex dielectric response in ceramics:

$$\varepsilon^*(\omega) = \varepsilon_\infty + \sum_{j=1}^{n} \frac{\omega_{pj}^2}{\omega_{oj}^2 - \omega^2 - i\gamma_j\omega} \qquad (3)$$

where $\varepsilon^*(\omega)$ is the compositive dielectric function; ε_∞ is the dielectric constant derived from the electronic polarization at a high frequency; ω_{pj} is the plasma frequency; ω_{oj} is the transverse frequency; γj is the damping factor of the j-th Lorentz oscillator; and n is the number of transverse phonon modes. The complex reflectivity R(ω) can be calculated with the following formula [Eq. (4)]. [28]

$$R(\omega) = \left| \frac{1 - \sqrt{\varepsilon^*(\omega)}^2}{1 + \sqrt{\varepsilon^*(\omega)}^2} \right| \qquad (4)$$

Fig. 7 shows the calculated dielectric constant $\varepsilon'(\omega)$ and loss $\varepsilon''(\omega)$ gained from the fitted infrared reflectivity. When x is 0.2, the Bi$_{2/3}$MoO$_4$ ceramic is the primary component of the xNBM-(1-x)BMO ceramic. The calculated permittivity is similar to the measured value of the Bi$_{2/3}$MoO$_4$ ceramic. When x increases, the calculated permittivity has an increasing trend and is close to the measured value of the (NaBi)$_{0.5}$MoO$_4$ ceramic. However, all the calculated values are inferior to the measured one at the microwave frequency, and the loss is inversely related to the dielectric constant and is slightly higher than the measured one. These results infer that the phonons in infrared regions lead to the polarization response of xNBM-(1-x)BMO ceramics at the microwave frequency.

According to the XRD results, it is clearly seen that two phases coexist in the xNBM-(1-x)BMO ceramics. Hence, the theoretical densities of these composite ceramics are calculated by the following formula: [29]

$$\rho_t = \frac{\rho_1 v_1 + \rho_2 v_2}{v_1 + v_2} \qquad (5)$$

where ρ_1 and ρ_2 are the theoretical densities of the independent
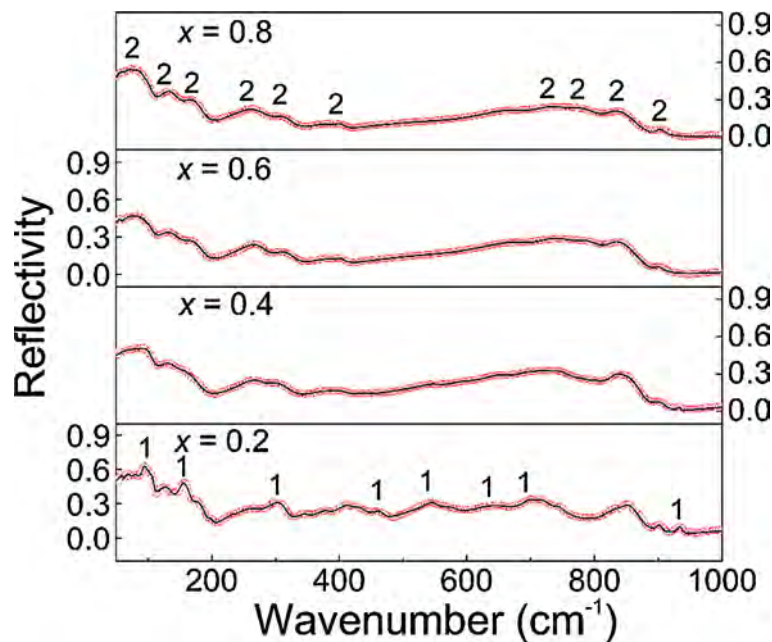
Fig. 6. The infrared reflectivity spectra of xNBM-(1-x)BMO ($x = 0.2 \sim 0.8$) ceramics (solid line is fitting value and red circle is measured value), (1 belongs to the vibration peak of $Bi_{2/3}MoO_4$ and 2 belongs to the vibration peak of $(NaBi)_{0.5}MoO_4$).

ceramics and v_1 and v_2 are the volume fractions of $(NaBi)_{0.5}MoO_4$ and $Bi_{2/3}MoO_4$, respectively. According to the literatures [24,25], the theoretical density of the $(NaBi)_{0.5}MoO_4$ ceramic is 5.69 g/cm^3, and the $Bi_{2/3}MoO_4$ ceramic is 6.19 g/cm^3. When x value increases, the total theoretical density has a falling off trend. Based on the measured densities (ρ_m) and theoretical densities (ρ_t), the relative densities (ρ_r) of xNBM-(1-x)BMO ceramics can be calculated using the following formula: [30]

$$\rho_r = \frac{\rho_m}{\rho_t} \times 100\%$$

(6)

The bulk densities, relative densities and sintering temperatures of the xNBM-(1-x)BMO ceramics are shown in Fig. 8(a). The measured densities have the same change trend as the theoretical densities. When the x value is 0.2, the phase of the $Bi_{2/3}MoO_4$ ceramic dominates, the total bulk density is 5.98 g/cm^3, and the total theoretical density is 6.09

g/cm^3. When x value is 0.8, the $(NaBi)_{0.5}MoO_4$ phase dominates and the equivalent bulk density decreases to 5.41 g/cm^3. Meanwhile, the equivalent theoretical density also decreases to 5.74 g/cm^3. From previous reports [31,13], the sintering temperature of the $(NaBi)_{0.5}MoO_4$ ceramic is higher than that of the $Bi_{2/3}MoO_4$ ceramic, and the optimal sintering temperature of xNBM-(1-x)BMO ceramics has an upward tendency with an increasing x value.

The ε_r value, Qf value and τ_f value of the xNBM-(1-x)BMO ceramics are shown in Fig. 8(b). Due to the higher permittivity of $(NaBi)_{0.5}MoO_4$ ceramic, the permittivity of the composite ceramics increases from 23.7–33.2. The Qf value is related to the dielectric losses. Many defects, such as pores, secondary grains, and particle sizes, indirectly impact the dielectric loss [32,33]. Hence, the high Qf values of microwave ceramics can be achieved only over a narrow sintering temperature range. For the xNBM-(1-x)BMO ceramics, stable Qf values were obtained in
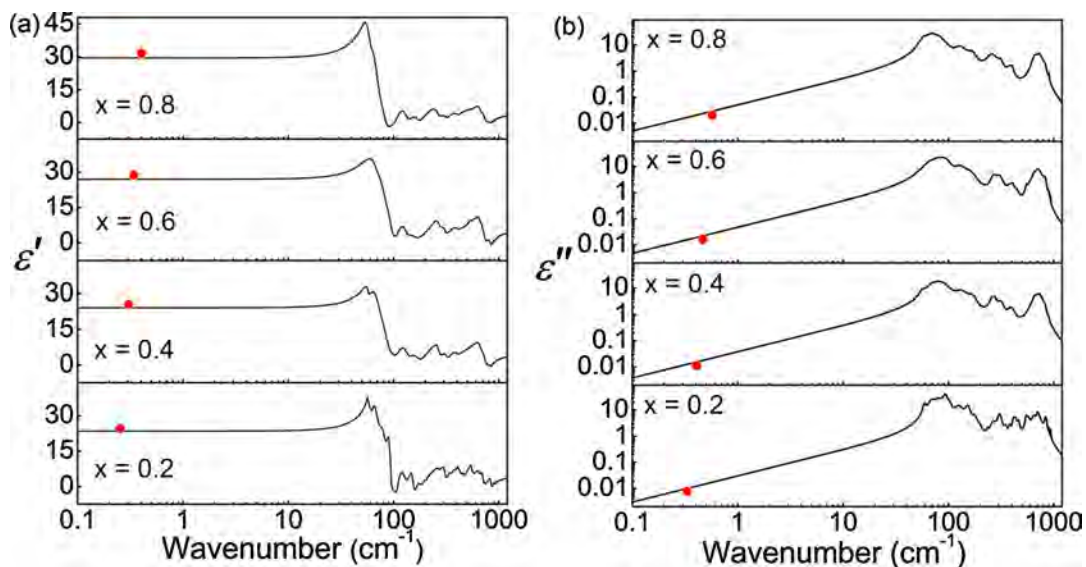
Fig. 7. (a) measured permittivity (red circle) and calculated permittivity ε'(ω), (b) measured dielectric loss (red circle) and calculated dielectric loss ε"(ω) of xNBM-(1-x)BMO ($x = 0.2 \sim 0.8$) ceramics.
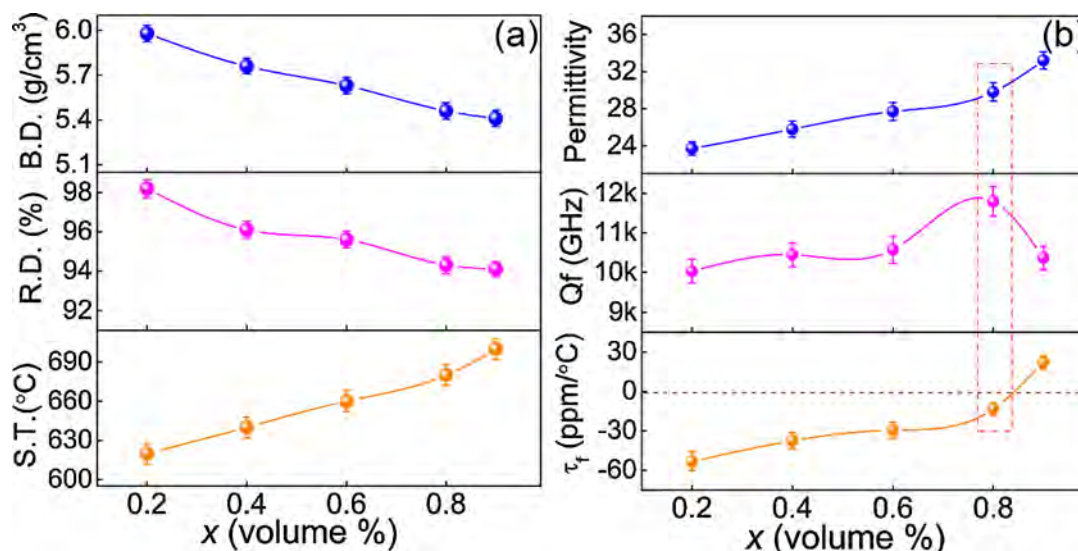
Fig. 8. (a) the bulk density, relative density and sintering temperature, (b) permittivity, Qf value and τ_f value of the xNBM-(1-x)BMO (x = 0.2 ~ 0.8) ceramics.

Table 1
Microwave dielectric properties of the low temperature ceramics sintered at different sintering temperatures.

Compound	S.T(°C)	ε_r	Qf(GHz)	τ_f(ppm/°C)	Ref.
$(Na_{0.5}Bi_{0.5})_{0.6}Ca_{0.4}MoO_4$	750	21.9	20,060	+8.4	[34]
$(AgBi)_{0.5}MoO_4$	660	27.7	10,577	−29.5	[18]
$(AgBi)_{0.5}(MoW)_{0.5}O_4$	580	26.7	10,000	+20	[35]
$0.8(NaBi)_{0.5}MoO_4$-$0.2Bi_{2/3}MoO_4$	680	29.8	11,800	−13.4	This work
$0.15TiTe_3O_8$-$0.85TeO_2$	670	30	22,000	−19	[36]
Bi_2TiTeO_8	840	36	4700	+47	[37]
$(KBi)_{0.5}MoO_4$	630	37	4,000	+117	[18]
$Bi_2Te_2O_8$	650	39	23,000	−43	[12]

ceramics sintered at 620 ~ 680 °C. Moreover, when τ_f is close to zero, microwave devices made from microwave materials can be applied at different working temperatures. When the x value increases from 0.2 to 0.8, the τ_f value shifts from -53.3 ppm/°C to +22.1 ppm/°C. The best microwave dielectric properties were obtained in the 0.8NBM-0.2BMO ceramic sample sintered at 680 °C for 2 h with a relative permittivity of 29.8, a Qf value of 11,800 GHz and a τ_f value of -13.1 ppm/°C. Similar low-temperature ceramic compounds with different sintering temperatures (S.T) and microwave dielectric properties (relative permittivity, Qf value, τ_f value) are summarized in Table 1 [12,18,34–37]. Compared to these results, the 0.8NBM-0.2BMO ceramic in our work showed a great overall microwave dielectric performance, which could be considered as a promising candidate in LTCC technology.

4. Conclusion

In summary, based on the Na_2O-Bi_2O_3-MoO_3 ternary phase diagram, the xNBM-(1-x)BMO (x = 0.2 ~ 0.8) composite ceramics are successfully prepared. The two coexisting phases are confirmed using XRD data and Raman analysis. From the BEI micrographs and EDS analysis, a partial solid solution is present in the 0.8NBM-0.2BMO ceramic. From the measurement of densities, the bulk densities of the composite ceramics have an increasing trend. From the measurement of microwave dielectric properties, the dielectric constant maintains an upward trend, which is attributed to the increase of $(NaBi)_{0.5}MoO_4$ phase with a high permittivity. However, the quality factor has a small change, which means that the component contents of the two phases have minimal effects on the dielectric loss in xNBM-(1-x)BMO ceramics. Favourable microwave dielectric properties with ε_r = 29.8 (6.7 GHz),

Qf = 11,800 GHz and τ_f = -13.7 ppm/°C were obtained in the 0.8NBM-0.2BMO ceramic. Considering that the sintering temperature is 680 °C, this ceramic has good potential for application in LTCC technology.

Declaration of Competing Interest

The authors declare no conflicts of interest.

Acknowledgments

References

[1] H.T. Yu, J.S. Liu, W.L. Zhang, S.R. Zhang, Ultra-low sintering temperature ceramics for LTCC applications: a review, J. Mater. Sci. Mater. Electric. 12 (2015) 9414–9423.

[2] M.T. Sebastian, H. Wang, H. Jantunen, Low temperature co-fired ceramics with ultra-low sintering temperature: a review, Curr. Opin. Solid State Mater. Sci. 3 (2016) 151–170.

[3] I.M. Reaney, D. Iddles, Microwave dielectric ceramics for resonators and filters in mobile phone networks, J. Am. Ceram. Soc. 7 (2006) 2063–2072.

[4] D. Zhou, L.X. Pang, D.W. Wang, C. Li, B.B. Jin, I.M. Reaney, High permittivity and low loss microwave dielectrics suitable for 5G resonators and low temperature co-fired ceramic architecture, J. Mater. Chem. C 5 (2017) 10094–10098.

[5] E.G. Larsson, O. Edfor, F. Tufvesson, T.L. Marzetta, Massive MIMO for next generation wireless systems, IEEE Commun. Mag. 52 (2014) 186–195.

[6] H.H. Guo, D. Zhou, L.X. Pang, Z.M. Qi, Microwave dielectric properties of low firing temperature stable scheelite structured (Ca, Bi)(Mo, V)O₄ solid solution ceramics for LTCC applications, J. Eur. Ceram. Soc. 39 (2019) 2365–2373.

[7] H.H. Guo, D. Zhou, W.F. Liu, L.X. Pang, D.W. Wang, J.Z. Su, Z.M. Qi, Microwave dielectric properties of temperature-stable zircon-type (Bi, Ce)VO₄ solid solution ceramics, J. Am. Ceram. Soc. 103 (2020) 423–431.

[8] G.H. Chen, J.C. Di, H.R. Xu, M.H. Jiang, C.L. Yuan, Microwave dielectric properties of Ca₄La₂Ti₅₋ₓ(Mg₁/₃Nb₂/₃)ₓO₁₇ ceramics, J. Am. Ceram. Soc. 95 (2012) 1394–1397.

[9] W. Lei, Z.Y. Zou, Z.H. Chen, B. Ullah, A. Zeb, X.K. Lan, W.Z. Lu, G.F. Fan, X.H. Wang, X.C. Wang, Controllable τ_f value of barium silicate microwave dielectric ceramics with different Ba/Si ratios, J. Am. Ceram. Soc. 101 (2018) 25–30.

[10] H.H. Guo, D. Zhou, C. Du, P.J. Wang, W.F. Liu, L.X. Pang, Q.P. Wang, J.Z. Su,

C. Singh, S. Trukhanov, Temperature stable $Li_2Ti_{0.75}(Mg_{1/3}Nb_{2/3})_{0.25}O_3$-based microwave dielectric ceramics with low sintering temperature and ultra-low dielectric loss for dielectric resonator antenna applications, J. Mater. Chem. C (2020), https://doi.org/10.1039/d0tc00326c.

[11] H.C. Xiang, C.C. Li, Y. Tang, L. Fang, Two novel ultralow temperature firing microwave dielectric ceramics $LiMVO_6$ (M = Mo, W) and their chemical compatibility with metal electrodes, J. Eur. Ceram. Soc. 37 (2017) 3959–3963.

[12] M. Udovic, M. Valant, D. Suvorov, Phase formation and dielectric characterization of the Bi_2O_3-TeO_2 system prepared in an oxygen atmosphere, J. Am. Ceram. Soc. 87 (2004) 591–597.

[13] D. Zhou, H. Wang, L.X. Pang, C.A. Randall, X. Yao, Bi2O3-MoO3 binary system: an alternative ultralow sintering temperature microwave dielectric, J. Am. Ceram. Soc. 92 (2009) 2242–2246.

[14] E.S. Kim, C.J. Jeon, P.G. Clem, Effects of crystal structure on the microwave dielectric properties of ABO_4 (A= Ni, Mg, Zn and B= Mo, W) Ceramics, J. Am. Ceram. Soc. 95 (2012) 2934–2938.

[15] D. Zhou, L.X. Pang, J. Guo, G.Q. Zhang, Y. Wu, H. Wang, X. Yao, Low temperature firing microwave dielectric ceramics $(K_{0.5}Ln_{0.5})MoO_4$ (Ln= Nd and Sm) with low dielectric loss, J. Eur. Ceram. Soc. 31 (2011) 2749–2752.

[16] A. Surjith, R. Ratheesh, High Q ceramics in the $ACe_2(MoO_4)_4$ (A= Ba, Sr and Ca) system for LTCC applications, J. Alloys Compd. (2013) 169–172.

[17] D. Zhou, W.B. Li, J. Guo, L.X. Pang, Z.M. Qi, T. Shao, H.D. Xie, Z.X. Yue, X. Yao, Phase evolution, and microwave dielectric properties of $(Ag_{0.5}Bi_{0.5})(Mo_{0.5}W_{0.5})O_4$ ceramic with ultralow sintering temperature, Inorg. Chem. 53 (2014) 5712–5716.

[18] D. Zhou, C.A. Randall, L.X. Pang, H. Wang, J. Guo, G.Q. Zhang, Y. Wu, K.T. Guo, L. Shui, X. Yao, Microwave dielectric properties of $(ABi)_{1/2}MoO_4$ (A= Li, Na, K, Rb, Ag) type ceramics with ultra-low firing temperatures, Mater. Chem. Phys. 129 (2011) 688–692.

[19] J. Guo, A.A. Sobol, P.G. Zverev, L.I. Ivleva, V.V. Osiko, R.C. Powell, Raman spectroscopy of crystals for stimulated Raman scattering, Opt. Mater. 11 (1999) 307–314.

[20] T.T. Basiev, A.A. Sobol, Yu.K. Voronko, P.G. Zverev, Spontaneous Raman spectroscopy of tungstate and molybdate crystals for Raman lasers, Opt. Mater. 15 (2000) 205–216.

[21] R.K. Khanna, E.R. Lippincott, Infrared spectra of some scheelite structures, Spectrochim. Acta Part A 24 (1968) 905–908.

[22] G.M. Clark, W.P. Doyle, Infra-red spectra of anhydrous molybdates and tungstates, Spectrochim. Acta 22 (1966) 1441–1447.

[23] G.Q. Zhang, H. Wang, J. Guo, L. He, D.D. Wei, Q.B. Yuan, Ultra-low sintering temperature microwave dielectric ceramics based on Na_2O-MoO_3 binary system, J. Am. Ceram. Soc. 98 (2015) 528–533.

[24] R.G. Teller, Refinement of some $Na_{0.5-x}M'_{0.5+x/3}\square_{2x/3}MoO_4$, M'= Bi, Ce, La, scheelite structures with powder neutron and X-ray diffraction data, Acta. Crystallogr. Sec. C Cryst. Struct. Commun. 48 (1992) 2101–2104.

[25] A.F. Van den Elzen, G.D. Rieck, The crystal structure of $Bi_2(MoO_4)_3$, Acta Crystallogr. Sect. B Struct. Crystallogr. Cryst. Chem. 29 (1973) 2433–2436.

[26] D. Zhou, L.X. Pang, H. Wang, J. Guo, X. Yao, C.A. Randall, Phase transition, Raman spectra, infrared spectra, band gap and microwave dielectric properties of low temperature firing $(Na_{0.5x}Bi_{1-0.5x})(Mo_xV_{1-x})O_4$ solid solution ceramics with scheelite structures, J. Mater. Chem. 21 (2011) 18412–18420.

[27] J. Hanuza, M. Mączka, L. Macalik, J. van der Maas, Polarized Raman spectra of $NaBi(MoO_4)_2$ crystal and order-disorder effect in solid scheelites, J. Mol. Struct. (1994) 119–124.

[28] K. Fukuda, R. Kitoh, I. Awai, Far-infrared reflection spectra of dielectric ceramics for microwave applications, J. Am. Ceram. Soc. 77 (1994) 149–154.

[29] C.L. Huang, M.H. Weng, Improved high Q value of $MgTiO_3$-$CaTiO_3$ microwave dielectric ceramics at low sintering temperature, Mater. Res. Bull. 36 (2001) 2741–2750.

[30] Q.W. Liao, L.X. Li, X. Ren, X. Ding, New low-loss microwave dielectric material $ZnTiNbTaO_8$, J. Am. Ceram. Soc. 94 (2011) 3237–3240.

[31] W.B. Li, D. Zhou, H.H. Xi, L.X. Pang, X. Yao, Structure, infrared reflectivity and microwave dielectric properties of $(Na_{0.5}La_{0.5})MoO_4$-$(Na_{0.5}Bi_{0.5})MoO_4$ ceramics, J. Am. Ceram. Soc. 99 (2016) 2083–2088.

[32] M.Z. Hu, H.S. Gu, X.C. Chu, J. Qian, Z.G. Xia, Crystal structure and dielectric properties of $(1-x)Ca_{0.61}Nd_{0.26}TiO_3 + xNd(Mg_{1/2}Ti_{1/2})O_3$ complex perovskite at microwave frequencies, J. Appl. Phys. 104 (2008) 124104.

[33] D. Zhou, L.X. Pang, X. Yao, H. Wang, Influence of sintering process on the microwave dielectric properties of $Bi(V_{0.008}Nb_{0.992})O_4$ ceramics, Mater. Chem. Phys. 115 (2009) 126–131.

[34] J. Guo, D. Zhou, Y. Li, T. Shao, Z.M. Qi, B.B. Jin, H. Wang, Structure-property relationships of novel microwave dielectric ceramics with low sintering temperatures:$(Na_{0.5x}Bi_{0.5x}Ca_{1-x})MoO_4$, Dalton Trans. 43 (2014) 11888–11896.

[35] D. Zhou, W.B. Li, J. Guo, L.X. Pang, Z.M. Qi, T. Shao, H.D. Xie, Z.X. Yue, X. Yao, Structure, phase evolution, and microwave dielectric properties of $(Ag_{0.5}Bi_{0.5})(Mo_{0.5}W_{0.5})O_4$ ceramic with ultralow sintering temperature, Inorg. Chem. 53 (2014) 5712–5716.

[36] M. Udovic, M. Valant, D. Suvorov, Dielectric characterisation of ceramics from the TiO_2-TeO_2 system, J. Eur. Ceram. Soc. 21 (2001) 1735–1738.

[37] M. Udovic, D. Suvorov, Sintering and dielectric characterization of pseudoternary compounds from the Bi_2O_3-TiO_2-TeO_2 system, J. Am. Ceram. Soc. 90 (2007) 2404–2408.